

Excitation-Emission fluorescence as a tool to assess the presence of grape-must caramel in PDO wine vinegars

Rocío Ríos-Reina^a, Juan A. Ocaña^b, Silvana M. Azcarate^c, Juan L. Pérez-Bernal^b, Mercedes Villar-Navarro^b, Raquel M. Callejón^{a*}

^aDpto. de Nutrición y Bromatología, Toxicología y Medicina Legal, Facultad de Farmacia, Universidad de Sevilla, C/P. García González nº2, E-41012 Sevilla, Spain

^bDepartamento Química Analítica, Facultad de Química, Universidad de Sevilla, C/P. García González s/n, E-41012 Sevilla, Spain

^c CONICET- Facultad de Ciencias Exactas y Naturales, Universidad Nacional de La Pampa, and Instituto de Ciencias de la Tierra y Ambientales de La Pampa (INCITAP), Santa Rosa, Argentina.

*rcallejon@us.es

Abstract

A practice in wine vinegar production is the addition of grape-must caramel to correct and unify the final colour of different batches. Although current legislation allows it, the effect in vinegars' quality has not been studied yet and it can become a fraud when it is used to simulate the effect of a longer ageing. Therefore, the aim of this work was to assess multidimensional fluorescence as a cost-effective and fast technique for detecting and quantifying grape-must caramel in vinegars. Different amounts of grape-must caramel and multivariate data analysis, as Parallel Factor Analysis (PARAFAC), N-way partial least squares and partial least squares discrimination and regression (NPLS-DA, PLS-DA and NPLS) were studied. Triangle sensory test was also performed. Results demonstrated the ability of this methodology in the detection and quantification of grape-must caramel (low prediction errors, RMSEP \approx 0.24) and the effects that grape-must caramel has upon a PDO vinegar's final quality.

Keywords: Wine vinegars, Protected Designation of Origin, Grape-must caramel, Fluorescence, Calibration, Classification.

1 1. INTRODUCTION

2 Wine vinegar is the most commonly-used vinegar in both Mediterranean countries and
3 Central Europe. Andalusia is a southern Spanish region traditionally associated with wine
4 growing where three high-quality wine vinegars have been protected under a legal
5 framework called Protected Designation of Origin (PDO): *Vinagre de Jerez*, *Vinagre de*
6 *Montilla-Moriles*, and *Vinagre de Condado de Huelva* PDOs (Council Regulation (EC) No
7 510/2006). These high-quality PDO wine vinegars are made from the corresponding
8 protected wines, endowing each vinegar with singular and specific characteristics. All of
9 the PDO regulations require an ageing period in wooden butts and during this ageing
10 period an important number of physicochemical changes take place. These changes are
11 what give the vinegars their unique organoleptic properties and sensory quality (Morales,
12 Tesfaye, García-Parrilla, Casas, & Troncoso, 2002). *Vinagre de Jerez* and *Vinagre de*
13 *Montilla-Moriles* PDOs have established the same categories regarding sweetness, time
14 and method of ageing (the *criaderas and solera* and *añada* system): *Pedro Ximenez*
15 category (sweet category), *Crianza* (aged in wood for at least 6 months), *Reserva* (with a
16 minimum ageing time of 2 years.) and *Gran Reserva* (aged for 10 or more years). During
17 ageing, the flavours of the barrel are absorbed by the vinegar and therefore, their quality
18 increases. This fact raises the final market price, thus making them more vulnerable to
19 frauds (Callejón et al., 2012). This means that PDO wine vinegar quality assurance and
20 authentication are highly important issues.

21 Authenticating and characterising PDO-labelled vinegars with the aim of assuring their
22 quality, is important for protecting the consumer against being sold an inferior quality or
23 counterfeit product (Danezis, Tsagkaris, Camin, Brusica, & Georgiou, 2016; Karoui & De
24 Baerdemaeker, 2007). The unfair activities related to high-quality wine vinegars that bear a
25 PDO label range from incorrect labelling to production outside PDO regulations or even to

26 adding substances prohibited by the regulations. One of the substances added to the
27 vinegars is grape-must caramel.

28 Grape-must caramel, also called 'grape syrup', is a sweetening and colouring agent
29 obtained after boiling the grape must which is very rich in sugars and is brown in colour
30 (Ortega-Heras & González-Sanjosé, 2009). It is commonly added to some Spanish wines
31 in order to obtain special sweet wines. The addition of grape-must caramel to Spanish
32 PDO wine vinegars is an allowed practice performed to unify the final colour of vinegars of
33 different batches. The amounts required for this purpose are low and they should not affect
34 the organoleptic characteristics of the final products. However, due to the fact that a
35 maximum limit of addition has not yet been established, this could lead to some
36 adulterations with the aim of modifying some of the characteristics of the final wine
37 vinegar.

38 During ageing the colour of wine vinegar changes from amber to mahogany. The content
39 and concentration of polyphenols, tannins and anthocyanins as well as an oxidation
40 process are the main factors involved in the vinegar's darkening. Many of these
41 compounds are also present in grape-must caramel, making determination of the
42 presence of grape-must caramel in vinegars a difficult issue. In this context, the addition of
43 grape-must caramel to the final wine vinegars could be used to simulate the effect of a
44 greater wood ageing in wine vinegars. It has been demonstrated that the addition of
45 grape-must caramel to a wine vinegar produces significant changes in its composition and
46 final characteristics with a large increase in both brown tonalities and sweetness (Ortega-
47 Heras & González-Sanjosé, 2009). Thus, the addition of grape-must caramel to a vinegar
48 could change its organoleptic characteristics, the final product being different from the raw
49 one. All of these facts illustrate the need for an analytical tool to determine and monitor the
50 addition of grape-must caramel to PDO-protected wine vinegars.

51 In recent years, interest has been growing in developing rapid, inexpensive, non-
52 destructive and direct methodologies based on non-targeted techniques for food
53 characterisation. In this context, today excitation-emission fluorescence spectroscopy has
54 an important role. Among the advantages of fluorescence spectroscopy is the enhanced
55 selectivity when compared to other spectroscopic techniques; its high sensitivity to a wide
56 range of potential analytes and an easy - or even unnecessary - sample pre-treatment
57 (Sayago, García-Gonzalez, Morales, & Aparicio, 2007). Fluorescence spectroscopy has
58 been applied as a competitive, high sensitivity, fast and non-destructive technique in food
59 analysis (Karoui & Blecker, 2011). In a previous study (Ríos-Reina et al., 2017) this
60 methodology demonstrated its usefulness for characterising and classifying PDO wine
61 vinegars

62 Measuring the emission spectra at different excitation wavelengths results in a three-
63 dimensional Excitation-Emission Matrix (EEM) array, which contains information unique to
64 each measured sample. Nowadays, the instrumental improvements and the availability of
65 software specially designed to extract information contained in spectra has enabled the
66 use of EEM in combination with chemometric methods in order to characterize and detect
67 adulteration in different matrices, such as different food products and beverages
68 (Azcarate, Teglia, Karp, Camiña, & Goicoechea, 2017; Casale et al., 2018;
69 Elcoroaristizabal et al., 2016; Öztürk, Ankan, & Özdemir, 2010; Sayago et al., 2007), as
70 well as in many other matrices (Heidari, Hemmateenejad, Yousefinejad, & Moosavi-
71 Movahedi, 2018; L. Zhu et al., 2016). The analytical information contained in fluorescence
72 spectra can be extracted in order better to interpret it using various multivariate analysis
73 techniques that relate several analytical variables to the analytes' properties. One
74 appropriate multiway method for extracting and interpreting the maximum information
75 possible from this matrix is PARAllel FACtor Analysis (PARAFAC). It has been applied in

76 order to break fluorescence EEMs down into different independent groups of fluorophores,
77 as well as their relative concentration (scores) in each sample (Bro, 1997). The information
78 provided by the resolved fluorophores has been successfully applied in food quality control
79 since it can reveal clearer insights into the relationships between the intrinsic food
80 properties and the quality of the product. Moreover, the extracted fluorophores could be
81 used for a classification approach by discriminant analytical methods such as partial least
82 squares-discriminant analysis (PLS-DA). In addition, the EEM array could also be studied
83 directly with the use of multivariate calibration methods such as N-way partial least
84 squares (N-PLS) that have also made it possible to relate instrument responses that
85 consist of several variables to a chemical or physical property of a sample, as well as with
86 multiway discrimination analysis such as NPLS-DA.

87 The aim of this study was to assess the potential of excitation-emission fluorescence
88 spectroscopy combined with three-way methods of analysis (PARAFAC and multiway N-
89 PLS regression) and discriminant analysis (PLS-DA and NPLS-DA) to detect and classify
90 the different additions of grape-must caramel in PDO wine vinegars. It is the first time that
91 a methodology for the determination of grape-must caramel has been established. Different
92 amounts of grape-must caramel were added to PDO wine vinegars that were grape-must
93 caramel free in their raw composition. In addition, commercial PDO wine vinegars (that
94 actually could have some added grape-must caramel) were also analysed to test the
95 models and to determine their amount of caramel. For this purpose, Parallel Factor
96 analysis (PARAFAC) was applied for pre-processing the three-dimensional arrays in order
97 to study the potential fluorophores related to this addition. Multivariate data analysis (PCA,
98 PLS-DA) was then performed in order to differentiate and classify samples that had or did
99 not have grape-must caramel in different concentrations. Consequently, the discrimination
100 results were compared to those obtained by a multiway partial least-squares discrimination

101 analysis (NPLS-DA). Finally, regression models were developed in order to attempt to
102 predict and quantify the level of grape-must addition by relating the PARAFAC
103 components to the chromatographic compounds detected, or by using the EEM array by
104 N-PLS regression method. Additionally, a sensory test was developed to evaluate the
105 influence of added grape-must caramel on the organoleptic properties of the PDO wine
106 vinegars and to propose a possible addition limit that does not affect or modify their unique
107 final organoleptic properties.

108 **2. MATERIALS AND METHODS**

109 **2.1. Samples**

110 Wine vinegar samples from two Spanish PDOs (*Vinagre de Jerez* and *Vinagre de*
111 *Montilla-Moriles*) were analysed in this study: 16 commercial wine vinegars from the
112 *Crianza* category (CR), aged for 6 months to 2 years (10 from *Vinagre de Jerez* PDO and
113 6 from *Vinagre de Montilla-Moriles* PDO) and 18 commercial wine vinegars from the
114 *Reserva* category (RE), aged from 2 to 10 years (13 from *Vinagre de Jerez* PDO and 5
115 from *Vinagre de Montilla-Moriles* PDO). These samples were collected working in
116 compliance with the Regulatory Councils and were grouped in this study as the
117 Unmodified group. Finally, 2 caramel-free samples of both *Crianza* and *Reserva* (one from
118 each PDO) were collected from the wineries and included in the study as Control samples.
119 More information and codification of samples is shown in Table 1.

120 **2.2. Reagents and Chemicals**

121 The grape-must caramel (also named colourant caramel MO-7) used was supplied by
122 SECNA S.A. (Valencia, Spain), with identification number CEE: E - 150 d. Water was
123 obtained from Milli-Q purification system (Millipore, USA). Analytical-quality acetic acid
124 and methanol were supplied by Merck (Darmstadt, Germany). 5-Hydroxymethylfurfural (5-

125 HMF) according to the standard OIV (2009) method was purchased from Sigma-Aldrich
126 (Madrid, Spain).

127 **2.3. Grape-must caramel addition**

128 First, thirteen different amounts of a dilution of grape-must caramel (10/100 v/v) were
129 added to 10 mL of vinegar: 5, 10, 20, 30, 40, 50, 75, 100, 125, 150, 175, 200, and 250 μL .
130 The amounts added were selected by examining the total range of colours of the
131 commercial wine vinegars. These samples were grouped into a class called Modified. The
132 vinegars selected as a matrix of these different additions were the *Crianza* and *Reserva*
133 vinegars without caramel in their composition collected directly from the winery and
134 belonging to both PDOs were designated as the Control samples. In table 1, therefore,
135 these samples appear in the Modified-control matrix group. Moreover, among these
136 samples made, five, with intermediate concentrations of grape-must caramel (20, 40, 75,
137 125, 175 μL), were used as the test set for assessing the robustness of the regression
138 models. These additions are expressed in Table 1 as % v/v.

139 In addition, and in order to include more samples in the models, the same procedure was
140 performed using a commercial *Crianza*-category wine vinegar from each PDO (also
141 grouped as Modified samples) by making 8 points of the above mentioned (group of
142 samples named in the study as Modified-Commercial matrix). Two replicates per level
143 were performed. A total of six curves were obtained by varying the matrix where the
144 grape-must caramel was added: 4 *Crianza* (two control and two commercial matrices) and
145 2 *Reserva* wine vinegars (control matrices). This information is more easily shown
146 schematically in Table 1.

147 Finally, the same calibration levels were performed in a hydroacetic matrix at 6% in order
148 to study the pure grape-must caramel. A schema and some photos of these curves are
149 shown in Supplementary Fig 1.

150 **2.4. Fluorescence analysis**

151 Fluorescence measurements were recorded using a Varian Cary-Eclipse fluorescence
152 spectrophotometer (Varian Iberica, Madrid, Spain), equipped with two Czerny-Turner
153 monochromators, and a Xenon discharge lamp pulsed at 80 Hz with a half peak height of
154 2 ms (peak power equivalent to 75 kW). A high-performance R298 photomultiplier tube
155 detector was used for collecting the fluorescence spectra. Wine vinegar samples were
156 analysed directly without sample pre-treatment by pipetting them into 3.5 mL quartz
157 cuvettes before measurement. 1-cm path length standard quartz cells (Hellma Analytics,
158 Müllheim, Germany) were used to perform the measurements in a Peltier thermostatic
159 cuvette holder (25.00 ± 0.05 °C). The spectrometer was interfaced to a computer with
160 Cary-Eclipse software for spectral acquisition and exportation.

161 The fluorescence Excitation-Emission Matrices (EEMs) were obtained by varying the
162 excitation wavelength (λ_{ex}) ranging between 250 and 650 nm (every 5 nm), and recording
163 the emission spectra (λ_{em}) from 300 to 700 nm (every 4 nm). For these measurements,
164 excitation and emission slits were both set at 5 nm, and the scan rate was fixed to 1200
165 nm min⁻¹. The system was wavelength-calibrated every day by means of the water Raman
166 peak to account for a possible instrument wavelength drift. EEMs were recorded in
167 triplicate for each wine vinegar type and each level of the calibration and pre-processed in
168 order to avoid noisy and non-informative areas by selecting shorter spectral ranges (λ_{ex}
169 from 300 to 650 nm, and λ_{em} from 300 to 700 nm).

170 **2.5. High-performance liquid chromatography (HPLC) analysis**

171 HPLC analysis was performed using a LaChrom® WWR-Hitachi (Barcelona, Spain) liquid
172 chromatograph with a quaternary L-7100 pump connected to an L-7455 diode array
173 detector (DAD). The column was a Luna C18, 5 µm, 250 x 4.6 mm and a guard precolumn
174 of 4.0 x 3.0mm from Analytical Phenomenex (Torrance, CA, USA). Detection was
175 performed at 280 nm. The injection of the samples (10) µL was performed using an L-
176 2200 autosampler and the separation was obtained at a flow rate of 1.2 mL min⁻¹ with an
177 isocratic elution. The analysis takes less than five minutes.

178 The mobile phase consisted of 80% water, 18% methanol and 2% acetic acid- Previously
179 filtered through a 0.45 µm PTFE membrane filter (Merck, Darmstadt, Germany), the
180 samples were analysed in duplicate. Quantification of 5-HMF was performed according to
181 Elcoroaristizabal et al., 2016, by using an external calibration curve in the range between 5
182 and 80 ppm. A calibration curve at 6 levels with two replicates per level was built using the
183 least-squares method. The response of the 5-HMF standard was linear within the
184 concentration range tested, with a determination coefficient of $R^2 = 0.997$. Standard
185 solutions were prepared using a hydro-acetic matrix (6% v/v).

186 **2.6. Sensory analysis**

187 An olfactory and taste analysis was carried out. The expert sensory panel comprised eight
188 tasters (six females and two male), all belonging to our laboratory and with extensive
189 experience in wine vinegar sensory analysis. For the olfactory test, fifteen millilitres of
190 each sample were presented in coded opaque glasses to mask the colour while following
191 the protocol for vinegars established by Tesfaye et al., 2010. For the gustative test, a drop
192 of each sample was placed in a coffee spoon.

193 Firstly, an ascending order test was performed to delimit the correct concentration range
194 of grape-must caramel to study and to familiarize panellists with the odour of the samples.

195 Panellists were asked to indicate in which glass and spoon they perceived any change of
196 odour or flavour. The starting point was the CR control without any caramel. Secondly,
197 triangular tests (ISO 4120 - 1983) were performed to ascertain whether the panellists were
198 capable of discriminating caramel-free samples from those vinegars with added grape-
199 must caramel. Moreover, triangle tests were also performed to assess the capability of
200 discriminating some *Reserva* commercial wine vinegars from the modified wine vinegars
201 from each PDO.

202 **2.7. Software and data analysis**

203 **2.7.1. Pre-processing of spectra and PARAFAC analysis**

204 EEMs data were pre-processed in order to correct Rayleigh and Raman scattering
205 (Elcoroaristizabal, Bro, García, & Alonso, 2015) by removing and replacing the scattering
206 areas with interpolated values by using the FLUCUT function included in the
207 PLS_Toolbox. The corrected EEM matrices underwent PARAllel FACtor analysis
208 (PARAFAC) (Bro, 1998) in order to extract the relevant information and to develop models
209 for differentiating authentic samples from those with added grape-must caramel. This
210 methodology is not described here due to having been described in a previous study
211 (Ríos-Reina et al., 2017). The number of factors for each model was determined by using
212 the CORe CONSistency DIAgnostic test (COR-CONDIA) (Bro & Kiers, 2003), the model
213 percentage of explained variance and by visual inspection of the recovered spectral
214 profiles and residuals. Non-negative constraints for all modes were applied.

215 **2.7.2. Exploratory and classification analysis**

216 **2.7.2.1. PCA and PLS-DA on the PARAFAC factors**

217 In order to perform a first screening of samples and to reflect the sample distribution in
218 latent space, principal component analysis (PCA) was applied to the scores of the

219 PARAFAC factors obtained. Moreover, classification accuracy was calculated by means of
220 Partial Least Squares-Discriminant Analysis (PLS-DA). This algorithm was used to build
221 classification models for discriminating the Unmodified (commercial) wine vinegar samples
222 from the Modified samples, that is, those CR and RE with the addition of grape-must
223 caramel and the control ones, in order to test the ability of the methodology to discriminate
224 between the presence or absence of grape-must caramel at different levels. Furthermore,
225 the data was autoscaled and samples were randomly divided into the training set
226 (comprising 75% of samples) that was used for data modelling and internal validation by
227 means of a venetian blinds cross-validation, and a test or prediction set used for
228 evaluating the discriminative power of the models (external validation).

229 **2.7.2.2. N-PLS discriminant analysis (NPLS-DA)**

230 NPLS-DA was applied to the three-dimensional array, which was prior multiway centred, in
231 order to compare the classification results of a multiway analysis to the previous one-way
232 approach (i.e. PLS-DA classification by the use of the PARAFAC factors). NPLS-DA is an
233 extension of PLS, used in the case of data in three-dimensional arrays. Thus, the NPLS-
234 DA consists of applying the N-PLS algorithm to classification, predicting the membership
235 of a sample to a qualitative group defined as a preliminary (Vigneau, Qannari, Jaillais,
236 Mazerolles, & Bertrand, 2006). In essence, N-PLS for discriminant analysis is the same as
237 for calibration purposes. Discrimination quality was obtained by comparing the predicted
238 groups to the real groups and is shown as the percentage of correct classification. The
239 data was again autoscaled and randomly divided again into two sample sets, as had been
240 the case with the PLS-DA model: the training set (comprising 75% of the samples) that
241 was used for calibration and internal validation of the models by means of a venetian
242 blinds cross-validation, and a test set used for evaluating the discriminative power of the
243 models employed as an external validation.

244 **2.7.3. Correlation of wine vinegars EEM spectra with grape-must caramel**

245 Regression models based on PARAFAC and N-PLS algorithms were compared. On the
246 one hand, the area of the compounds detected by HPLC as well as the % v/v of grape
247 must-caramel were correlated to the extracted PARAFAC components. On the other hand,
248 a multiway linear regression analysis, called N-way partial least squares (N-PLS), was built
249 using the EEM data which was multiway centred in order to determine the presence of
250 grape-must caramel in the commercial PDO wine vinegars by the fluorescence landscapes
251 kept as three-way array. Regression models were evaluated using the figures of merit:
252 Root Mean Square Error of calibration, cross-validation and prediction (RMSEC, RMSECV
253 and RMSEP) as a term to indicate the prediction error of the model, and the coefficient of
254 determination (R^2). R^2 , generally used for evaluating model quality, is the correlation
255 coefficient between the predicted and actual/measured grape-must caramel. RMSEC is
256 used to compare quality of the results provided in the calibrations and it is expressed as a
257 percentage (in both calibration and prediction), taking into account the response range in
258 its calculation (Sáiz-Abajo, González-Sáiz, & Pizarro, 2006). The data was multiway
259 centred across the first mode (i.e. sample mode) and divided into two sets, train and test.
260 Venetian blinds was applied by means of cross validation.

261 **2.7.4. Software**

262 EEM data modelling and chemometric analyses were performed by using the
263 PLS_Toolbox 7.9.5 (Eigenvector Research Inc., Wenatchee, WA) working under Matlab
264 v.8.5.0 environment (The Mathworks Inc., Natick, MA).

265 **3. RESULTS AND DISCUSSION**

266 **3.1. Visual assessment of fluorescence landscapes**

267 Fig. 1 shows, in the left side (a), an example of the fluorescence landscapes in the form of
268 contour plots (after removing and replacing the scattering areas) of different levels of the
269 calibration curve made with the *Crianza* Control wine vinegars as matrix (those without
270 caramel obtained from the wineries) from both PDOs, including also the *Reserva* Control
271 wine vinegars on the far right of the figure (Fig. 1a). Moreover, the calibration curve
272 produced with the hydroacetic matrix is also shown at the left bottom of the figure (Fig.
273 1c).

274 As can be observed, a visual assessment of the fluorescence landscapes indicated a
275 similar profile for vinegars of both PDOs, with fluorophores overlapping in both excitation
276 and emission dimensions, together with some differences due to the addition of grape-
277 must caramel. Thus, the fluorescence profiles of the *Crianza* vinegars without grape-must
278 caramel (first samples in the rows) showed a common maximum peak around 370/450 nm
279 for both excitation/emission wavelengths ($\lambda_{ex}/\lambda_{em}$), although in the *Reserva* control
280 samples (last samples in the rows) the maximum peaks appeared at slightly higher
281 wavelengths, around 370–470 nm of λ_{ex} and 470–550 nm of λ_{em} . These features were
282 similar to those observed in a previous work studying PDO wine vinegars (Ríos-Reina et
283 al., 2017).

284 Additionally, the visual assessment of the EEM landscapes with and without the addition
285 of grape-must caramel allows an *a priori* confirmation of differences between samples by
286 looking at the areas where the potential compounds appeared. Thus, for example, the
287 peak at 370/450 nm ($\lambda_{ex}/\lambda_{em}$) tended to disappear as more grape-must caramel was
288 added, giving way to the appearance of a second peak around 550/570 nm of excitation
289 and emission wavelength, respectively. It should be also noticed that, as the commercial
290 samples are able to present some grape-must caramel, some of the analyzed in this study
291 already showed this trend. Moreover, another important feature was that as more grape-

292 must caramel was added to the vinegar, EEM intensity decreased. This behaviour was
293 also observed as being PDO-independent - even in the hydroacetic matrix analysed (Fig.
294 1c). In fact, the hydroacetic samples with different amounts of grape-must caramel
295 showed similar trends, also being similar to the vinegar samples due to the fact that it
296 should be considered that grape-must caramel has many grape-derived compounds, such
297 as wine vinegars. However, the excitation/emission wavelengths were not exactly the
298 same, due to the relevant phenomena related to the nature of the food and its molecular
299 environment, both of which influence the fluorescence signal. This is commonly called the
300 matrix effect (Azcarate et al., 2017). All of these results partially demonstrated that
301 excitation-emission fluorescence was able to detect those samples whose colour was
302 modified by the addition of grape-must caramel.

303 **3.2. Decomposition of the spectral data in the potential fluorophores by using** 304 **PARAFAC**

305 In order to observe and evaluate the pure spectra of fluorophores related to the addition of
306 grape-must to wine vinegars, an adequate multiway method for pre-processing the three-
307 dimensional array was carried out. Thus, the EEM landscapes of all of the samples under
308 study (the Modified and the Unmodified samples of both categories and both PDOs) were
309 decomposed into the main fluorescence contributions by using PARAFAC analysis. The
310 best PARAFAC model built for each PDO was obtained with five factors, giving final
311 reliable models that explain more than 99% of the variance and with a core consistency
312 over zero. Fig. 1 also shows in the right side the PARAFAC loadings (excitation/emission
313 profiles) of each main fluorophore obtained for both PDOs (Fig. 1b) and hydroacetic matrix
314 with different amounts of grape-must caramel (Fig. 1d). A great similarity of the spectral
315 profiles acquired for both PDOs (*Vinagre de Jerez* in discontinuous lines and *Vinagre de*
316 *Montilla-Moriles* in continuous lines) could be observed. This fact suggests that these

317 fluorescence fingerprints could be useful for addressing the problem under study, as it
318 shown to be PDO-independent. Similar results were obtained by Elcoroaristizabal et al.,
319 (2016) in the study of different types of Cava in which a great similarity of the spectral
320 profiles was obtained independently of the Cava analysed.

321 The fluorescent loading patterns of the modelled factors in the PDO samples can be
322 matched to fluorophores described in the literature. The first factor (F1, blue in Fig. 1b)
323 therefore, has a similar profile for the two PDOs under study with excitation and emission
324 maxima centred around 380 nm and 450 nm, respectively. This factor also appeared in the
325 previous study (Ríos-Reina et al., 2017) and was related to the cumarins, tannins,
326 phenols, flavonols that are naturally present in wine.

327 The second factor (F2, red in Fig. 1b) is a peak centred at 400-430nm of excitation and
328 500-520 nm of emission. This fluorophore could be matched with Maillard compounds
329 according to Zhu, Ji, Eum, & Zude (2009) and Ríos-Reina, et al. (2017), formed in
330 vinegars during ageing (García Parrilla, Heredia, & Troncoso, 1999). According to the
331 literature, within these compounds, 5-HMF is one that has been shown to have a high
332 correlation to these wavelengths (Callejón et al., 2012). Grape-must caramel also has high
333 amounts of this compound. In this regard, it is important to emphasize that each
334 PARAFAC factor probably corresponds to a related fluorescent molecule group, and not
335 necessarily to a single fluorescent molecule and for that reason, this factor could be
336 matched with different compounds, although from a similar family.

337 The third factor (F3, yellow in Fig. 1b) shows an excitation maximum around 470 and the
338 emission one at 550 nm for both PDOs although for *Vinagre de Jerez* this factor shows a
339 shoulder at 350 nm of excitation that could be due to differences in the composition
340 between the two PDOs. According to the literature (Airado-Rodríguez, Durán-Merás,
341 Galeano-Díaz, & Wold, 2011) and our previous knowledge (Ríos-Reina et al., 2017), the

342 common parts of this factor appeared to be related to vitamin B2 and its principal forms
343 such as Riboflavin, Flavin mononucleotide (FMN), and Flavin adenine dinucleotide (FAD)

344 The fourth factor (F4, purple in Fig. 1b) has excitation and emission maxima between 320-
345 340nm and 400-420 nm, respectively. In this case, the *Vinagre de Montilla-Moriles* factor
346 shows a small shoulder at 450 nm of emission, different to the other PDO. According to
347 the results presented in the literature, excitation/emission wavelengths around 330/420 nm
348 have been related to phenolic acids and phenolic aldehydes, as well as oxidation and
349 Maillard reaction products (present due to browning processes and oxidative mechanisms
350 taking place during ageing and storage) (Airado-Rodríguez et al., 2011; Azcarate et al.,
351 2015; Callejón et al., 2012; Dufour, Letort, Laguet, Lebecque, & Serra, 2006;
352 Elcoroaristizabal et al., 2016; Sádecká & Tóthová, 2007).

353 Finally, the fifth factor (F5, green in Fig. 1b) shows a peak centred at 550 nm of excitation,
354 with a shoulder at 400 nm in both PDOs, and an emission maximum around 600-630 nm.
355 This has not previously been associated to any fluorophore. However, this factor was
356 similar to the one obtained in the previous work (Ríos-Reina et al., 2017), which showed a
357 relationship to *Pedro Ximenez* wine vinegars. Consequently, higher mean values of this
358 factor were obtained for samples belonging to this category. The sweet category is
359 produced by adding raisined *Pedro Ximenez* grape must or adding *Pedro Ximenez* wine to
360 the vinegar. Therefore, the concentration of grape-must should be higher in these sweet
361 vinegars than in the *Crianza* or *Reserva* ones. For this reason, the presence of this factor
362 in our samples also appeared to be related to the addition of grape-must caramel, it being,
363 therefore, a relevant factor to take into account in this study.

364 As mentioned earlier, it is relevant to consider the phenomena related to the nature of the
365 food that will influence the fluorescence signal. These phenomena are related to the
366 inherent fluorophores' concentration and their environment. Therefore, a specific

367 fluorophore studied in different foods can present different spectral signals (Azcarate et al.,
368 2017). In fact, adding grape-must caramel changes the environment of the natural wine
369 vinegar fluorophores and so could have the ability to modify the signal, as can also be
370 observed in the 5-factor PARAFAC model of the hydroacetic matrix with only grape-must
371 caramel in its composition (Fig. 1d). Thus, the PARAFAC model built with the curve of
372 grape-must caramel in a hydroacetic matrix (Fig. 1d), shows similar fluorophores as in the
373 vinegar matrix, but some of them are displaced. In spite of this, the fifth factor (F5 in green,
374 Figure 1.d) matched perfectly in terms of excitation/emission wavelengths with the fifth
375 factor of the PARAFAC models developed with the PDO wine vinegars, which appeared to
376 have a strong relationship with the presence of grape-must caramel.

377 In fact, only the scores of the fifth PARAFAC factor (F5) extracted from the hydroacetic
378 curve showed an increase in the case of added grape-must caramel, appearing to follow a
379 logarithmic kinetic (Supplementary Fig. 3). Hence, the scores of the F5 described a
380 logarithmic kinetics equation as follows:

$$381 \quad Y = m \ln(Y_0) + b;$$

382 where Y is the score value of F5 (a.u.), m is the slope, Y_0 is the initial value of F5 score
383 (a.u.), and b the intercept. Thus, the logarithmic kinetic obtained with the fifth PARAFAC
384 factor, which is shown in Supplementary Fig. 3), was $Y = 42.538 \ln(Y_0) + 148.15$.

385 **3.3. Exploratory analysis**

386 A principal component model was developed with all of the Modified and Unmodified
387 samples for each PDO by using the extracted PARAFAC factors in order to explore the
388 data and to detect grouping and outliers in each PDO. The scores and loadings plots are
389 shown in Fig. 2. In general, a separation of both groups (modified and unmodified) could

390 be observed in the two PCA models for both PDOs, which means that the methodology
391 appeared to be able to detect the addition of grape-must caramel.

392 In the case of the *Vinagre de Montilla-Moriles* PCA model (Fig. 2a), the first component
393 (PC1) is the main factor in the separation, explaining 69.30% of the original variance,
394 showing a good separation of the groups, the modified samples being located on the
395 negative side of PC1 and the unmodified on the positive side. However, it was also
396 observed that three unmodified samples (i.e. commercial samples) were grouped closely
397 to the modified ones, especially two RE samples located next to the samples containing
398 the most added grape-must caramel. These results suggest that these two RE samples
399 could have a higher amount of grape-must caramel in their composition than the other
400 commercial samples, something that could change the raw organoleptic characteristics by
401 binding the effect of some compounds related to ageing; or it could even be a case of
402 unfair practice, these RE samples in fact being CR vinegars with added grape-must
403 caramel in order for them to resemble the colour of an RE.

404 With regard to the Modified samples, those with the lowest amounts of grape-must
405 caramel (lower than 0.1% v/v) were located near to some commercial samples. Thus, a
406 commercial *Crianza* sample was observed located very close to a Modified wine vinegar in
407 the scores plot, this modified sample being a *Crianza* Control vinegar containing 0.05%
408 grape-must caramel. These results showed that some commercial samples could have a
409 very low amount of grape-must caramel in their final composition. In terms of the loadings
410 plot, and due to its position on the plot, the fifth factor once again appeared to be the
411 greatest factor regarding the presence of grape-must caramel, followed by F4.

412 With regards to the PCA model of *Vinagre de Jerez* (Fig. 2b), the separation in this
413 particular case appeared to be more related to PC3. Thus, observing the scores plot of
414 PC1 vs PC3, modified samples were located on the negative side of PC3, although once

415 again, a few unmodified samples (some CR and RE commercial samples) were not
416 properly separated from the modified ones in this model. As before, this placement could
417 be explained by a greater amount of grape-must caramel in their composition than the rest
418 of samples, thus affecting the composition by binding some relevant compounds. These
419 wrongly-placed RE commercial samples therefore appeared to have more similarities
420 according to their scores with the RE samples modified with 1-2.5% v/v of grape must
421 caramel, as well as the fact that the aforementioned wrongly-placed CR commercial
422 samples appeared to be more similar to the CR samples modified with 1.5-2% v/v of
423 grape-must caramel.

424 The separation of both groups of samples was again explained by the F5, as could be
425 observed in the loadings plot. However, when observing the loadings plot, F4 and F1 also
426 appeared to play an important role in this separation. This partially agrees with the results
427 mentioned above (Section 3.1) in which F4 was related to Maillard reaction products that
428 could be derived from the grape-must caramel.

429 **3.4. Classification analysis of modified (by adding grape-must caramel) and** 430 **unmodified samples (commercial wine vinegars)**

431 Once the ability of the multidimensional fluorescence spectroscopy in distinguishing the
432 presence of grape-must caramel at different levels was demonstrated, the next step was to
433 gain an insight into this differentiation and to determine if the extracted PARAFAC
434 fluorophores allows the classification of samples according to the modification of vinegars
435 with grape-must caramel. To this end, PLS-DA classification models were performed using
436 the extracted PARAFAC factors. Moreover, in order to consider the contribution of multiple
437 effects and not only the most relevant information (PARAFAC factors), NPLS-DA
438 classification models were also performed, taking the multiway arrays (EEMs) into
439 consideration. Both classification models were therefore studied and compared in the

440 following section. Prior to the classification analysis, the data set was randomly partitioned
441 into two sets, train and test, and all of the datasets were mean-centred before developing
442 the models.

443 **3.4.1. PLS-DA classification between modified and unmodified wine** 444 **vinegars using the extracted PARAFAC factors.**

445 Two PLS-DA models were developed according to each PDO including samples from the
446 two groups in the train and test sets. The *Vinagre de Jerez* PLS-DA model was obtained
447 using 4 latent variables (LVs), which explained 99.75% of total variance, while the PLS-DA
448 model of *Vinagre de Montilla-Moriles* was obtained using 3 LVs and explained 96.83% of
449 total variance. Table 2 shows the PLS-DA classification results expressed as the
450 percentage of correct classification and the number of samples misclassified for each
451 class. Additionally, the statistical performance parameters of the classification models (i.e.
452 sensitivity, specificity and classification error of calibration (CAL), cross-validation (CV) and
453 prediction (PRED)) are shown in Supplementary Table 1. Correct classification rates of
454 100% were obtained for both Modified and Unmodified groups in the training set for each
455 PDO. In this way it was observed that the models were able to classify the unmodified
456 samples, where both CR and RE commercial samples are grouped, from those modified
457 with the addition of grape-must caramel. To test the models, those commercial samples
458 that were not well-located on the previous exploratory models were purposely included in
459 the prediction sets, together with other unmodified and modified samples in order not to
460 disturb the model's calibration. The classification results enabled the results observed by
461 the previous PCA models to be confirmed, since the seven misclassified samples were
462 those that behaved differently to the rest of commercial PDO wine vinegars.

463 Moreover, the classification results showed that a 100% correct classification was
464 achieved for all of the modified samples for the prediction set, confirming the good

465 predictive ability of the classification models developed and, hence, multidimensional
466 fluorescence spectroscopy's ability to detect the addition of grape-must caramel to wine
467 vinegars.

468 Furthermore, the possibility of taking both PDOs into account together was tested. Table 2
469 shows that the PLS-DA model obtained with 5 latent variables and 99.64% of total
470 variance explained, again classified the same seven unmodified samples as modified wine
471 vinegars. However, in spite of the fluorescent components appearing to be very similar in
472 both PDOs, when a classification is performed by including both PDOs together, the
473 percentage of correct sample classification was lower than in the separated models.

474 **3.4.2. NPLS-DA classification between modified and unmodified wine** 475 **vinegars using the three-dimensional arrays EEM.**

476 Once again it should be emphasised that each factor probably does not necessarily
477 correspond to a single fluorescent molecule (Elcoroaristizabal et al., 2016). It is, therefore,
478 possible that different factors need to contribute in order to explain a group of compounds.
479 For this reason, a multiway classification approach was studied. In this case the three-
480 dimensional arrays (EEMs) were used, NPLS-DA was performed and their results were
481 compared to those obtained by PLS-DA with the PARAFAC factors. NPLS-DA
482 classification results are also shown in Table 2. In addition, the statistical performance
483 parameters of the NPLS-DA classification models are shown in Supplementary Table 1. It
484 can be seen that a highly discriminant NPLS-DA model was obtained by using three PLS
485 factors for both *Vinagre de Jerez* and *Vinagre de Montilla-Moriles* models. Here, and
486 similar to the previous PLS-DA results, six commercial samples (three of *Vinagre de Jerez*
487 and three of *Vinagre de Montilla-Moriles*) were classified as being modified with grape-
488 must caramel. Moreover, the number of latent variables needed to explain the
489 classification, the percentage of total variance explained and the samples misclassified

490 (Table 2), as well as sensitivity and specificity (Supplementary Table 1), were almost the
491 same for the previously-discussed PLS-DA and the NPLS-DA models. As a result, both
492 approaches could be good options to consider. This could demonstrate that the
493 fluorophores extracted by PARAFAC were sufficient to explain the grape-must caramel
494 effect. However, although the multiway classification approach is faster and easier to
495 develop than undertaking PARAFAC and a PLS-DA, it provides less information with
496 respect to the fluorophores involved.

497 With regard to the model considering both PDOs together and obtained by 3 LVs, better
498 classification rates could be observed (higher percentage of correct classification and less
499 latent variables needed) for NPLS-DA than for the model obtained by PLS-DA and
500 PARAFAC factors, although, once again, the same seven commercial samples were
501 misclassified. This could be explained by the fact that in the multiway discrimination
502 methodology the whole fluorescence matrix is considered. This enables all of the
503 fluorophores related to caramel and to the effect of its environment to be modulated, as
504 well as being able to modulate the interferences.

505 **3.5. Correlation between the additions of grape-must caramel and EEMs.**

506 **3.5.1 Univariate calibration - HPLC analysis**

507 After confirming the changes in vinegar components observed in the EEMs with the
508 addition of grape-must caramel, and in order to ascertain the specific compound
509 concentrations which increase or change with such an addition, a chromatographic
510 analysis was performed including the modified and unmodified samples, as well as the
511 hydroacetic solution (Fig. 3). In all of these analyses, three compounds were principally
512 observed to increase when grape-must caramel was added with the following elution order
513 (Fig. 3a): 2.3, 2.7 and 4.2 min of retention time. The first two compounds were
514 unidentified, whereas the last was identified by its corresponding standard as 5-

515 hydroxymethylfurfural (5-HMF). The 5-HMF and the compound termed as unknown 2,
516 (retention time at 2.7 min), presented in all of the samples, while unknown 1 (retention
517 time at 2.3 min) did not present in the wine vinegar matrices which had no grape-must
518 caramel in their raw composition (Control samples).

519 Some studies in the literature show that grape-must caramel has a high amount of
520 furfural-related compounds, including which 5-HMF (Ortega-Heras & González-Sanjosé,
521 2009). 5-HMF is a furanic compound formed during Maillard reactions or by direct
522 dehydration of sugars under acidic conditions (caramelisation) during thermal treatments
523 applied to foods (Capuano & Fogliano, 2011). Hence, its concentration should be high in
524 grape-must caramel. However, as can be observed in the calibration curves of the areas
525 of the three compounds and in the % of grape-must caramel (Fig. 3b), the compound that
526 presented the highest slope was the one named unknown2, and not, as expected, 5-HMF.
527 This could be explained by the fact that other compounds have been also determined in
528 the grape-must caramel and cooked musts, such as melanoidins, caramels (formed by
529 non-enzymatic browning reactions) and other furfurals (Ortega-Heras & González-
530 Sanjosé, 2009; Palacios, Valcarcel, Caro, & Perez, 2002), that could be related to the
531 unknown peaks detected. However, the structure of melanoidins is poorly defined and is
532 not isolated and characterised, making it difficult to identify them.

533 Regarding the commercial wine vinegars under study, especially those samples
534 misclassified as Modified samples which were expected to have a greater amount of
535 grape-must caramel in their composition, the chromatographic results agreed with the
536 fluorescence patterns. Hence, these samples showed higher areas of the two unknown
537 compounds and 5-HMF (i.e. three times more) than the rest of CR and RE commercial
538 wine vinegars.

539 **3.5.2 Multiway calibration**

540 In spite of the promising results shown in the previous section, as grape-must caramel is a
541 mixture of compounds and wine vinegar is another complex matrix of compounds, when a
542 univariate calibration was developed with PARAFAC components extracted from the wine
543 vinegar matrix, and not with the hydroacetic matrix, in this case satisfactory results were
544 not achieved. This could be explained by the fact that in order to make correct predictions
545 with the univariate model, the signal of the test samples can only vary due to the analyte,
546 so the contribution of the other species must be the same as what has been modelled. If
547 the contribution of these other species varies (because their concentration varies) or if
548 there is some new interfering signal, the prediction will be biased. The advantage of a
549 multiway calibration over the calibration line is that it allows selective information to be
550 obtained from non-selective instrumental responses (that is, in the presence of
551 interferences), thus enabling the determination of the concentration of various components
552 in complex samples (Olivieri, 2014) to be determined. By using multiway calibration, it has
553 been demonstrated that considerably more complex analytical problems can be solved
554 and predictions are possible - even in the presence of unexpected spectral interferences,
555 i.e., sample constituents not considered in the calibration phase (Arancibia, Damiani,
556 Escandar, Ibañez, & Olivieri, 2012; Bro, 1998; Christensen, Becker, & Frederiksen, 2005;
557 Olivieri, 2014; Olivieri & Escandar, 2014).

558 For this reason, a multiway calibration method such as N-PLS that considers the entire
559 EEM matrix was studied (Fig. 4). The N-PLS calibration model was built using the EEM
560 data from all of the modified and unmodified wine vinegars in an attempt to identify a
561 possible correlation of the matrices with the quantity of added grape-must caramel. This
562 algorithm has the advantage of being a simultaneous model, that is, all of the components
563 are extracted at the same time. Again, two strategies were developed: building a model
564 with both PDOs together, and analysing each PDO separately. The NPLS accuracy for

565 each model is shown in Fig. 4. As indicated by the high correlation coefficient ($R^2 > 0.921$)
566 and low RMSEC, the results of the three models were good. Moreover, the good
567 regression results obtained by the multiway calibration agree with those obtained by other
568 authors, due to the N-PLS algorithm having been demonstrated to be superior to unfolding
569 methods, primarily owing to a stabilisation of the decomposition that has been
570 demonstrated potentially to give better predictions (Bro, 1996). Moreover, another
571 advantage is that the algorithm is fast compared with the PARAFAC approach because it
572 consists of solving eigenvalue problems.

573 For regression model robustness, five of the modified samples prepared for each PDO
574 (with intermediate concentrations of 0.20, 0.40, 0.75, 1.25 and 1.75 % of grape must
575 caramel) were used as validation sets (included randomly in train and test) in order to test
576 the models using known amounts of grape-must caramel. The overall prediction model
577 accuracy obtained by the three NPLS models was very good with respect to the % of
578 grape-must caramel predicted for these 5 samples, demonstrating the efficacy of the
579 NPLS method. The results obtained, expressed as % of grape-must caramel, with the
580 predicted values in brackets, as follows: 0.2(0.29), 0.4(0.47), 0.75(0.93), 1.25(1.39), and
581 1.75(1.85) by the global model (being these values an average of the results for both
582 PDOs); 0.2(0.16), 0.4(0.58), 1.25(1.39), 1.75(1.74) for the *Jerez* model; and 0.2(0.18),
583 0.4(0.50), 0.75(0.99), 1.25(1.43) for the *Montilla-Moriles* model. The prediction results
584 obtained for the test set are shown in Supplementary Table 2. Therefore, regarding the
585 comparison between the measured and the predicted values obtained for these 5
586 samples, better results were obtained by the global NPLS model (with samples from both
587 PDOs) than by the individual NPLS model of each PDO. This might be explained by the
588 fact that this first model has a higher amount of samples with the same concentrations
589 than the individual models.

590 In terms of the real wine vinegars, the calibration results for the RE commercial samples of
591 both PDOs that had been shown as possibly containing more grape-must caramel or even
592 as being less aged vinegars, again agreed with the exploratory and classification analyses
593 performed in a previous section of this work. Thus, according to the predicted results
594 (Supplementary Table 2), the RE samples misclassified of *Vinagre de Jerez* PDO
595 presented amounts of grape-must caramel around 2.0%, agreeing with the predicted
596 values of modified samples with the addition of 2.0% of grape-must caramel, whereas the
597 rest of commercial samples had an amount of grape-must caramel lower than 1.5% and
598 even 0.0%. Regarding the RE samples of *Vinagre de Montilla-Moriles* PDO that were
599 classified as Modified, the predicted amount of grape-must caramel was higher than 1.0%,
600 while the rest of the commercial samples presented a predicted value of lower than 0.5%. 601
These values agreed totally with the observed trend of these samples in the previous PCA 602
models. These samples were also those that showed the highest chromatographic areas 603 for
the three selected peaks.

604 Furthermore, in CR commercial samples that also showed a high similarity to the Modified 605
samples with a lower amount of caramel (<0.05%), the percentages of grape-must 606
caramel obtained by the regression models were even negative, being in agreement with 607 this
assumption (Supplementary Table 2).

608 All of these results confirm the ability of this multiway calibration to determine the amount 609
of grape-must caramel in PDO wine vinegars and its ability to detect samples with an 610
excessively high concentration. An excessive addition of grape-must caramel to a vinegar 611 could
affect its quality due to sensory changes. In fact, ranking and triangle tests, both 612 gustatory
and olfactory, were undertaken in order to assess the hypothesis of the sensory 613 effect that
adding grape-must caramel could have and in order to know the specific level of 614 grape-must
caramel that modified the sensory characteristics. Thus, the results obtained

615 by these tests showed that, in general, 0.3% was the minimum level of concentration of 616 grape-must caramel at which all of the tasters perceived sensory differences in the 617 samples. However, in *Vinagre de Jerez*, grape-must caramel at a concentration of 0.05% 618 was also perceived by many testers as being different to the raw matrix. These results 619 reaffirm the relevance of the present study on the importance of quantifying the grape-620 must caramel added to wine vinegars, due to the fact that changes in the organoleptic 621 characteristics of wine vinegars were detected very low concentrations.

622 4 CONCLUSIONS

623 Multidimensional fluorescence coupled with a suitable chemometric method has shown 624 itself to be a valuable tool for detecting and, for the first time, quantifying the addition of 625 grape-must caramel to wine vinegars without sample treatment. Thus, the methodology 626 proposed provided results that were in agreement with those obtained by the conventional 627 HPLC analytical method. This, therefore, demonstrated the validity of the procedure for 628 determining the amount of grape-must caramel in wine vinegars.

629 This study has also shown that the multiway regression and classification approaches 630 using NPLS and NPLS-DA, respectively, provide even better results more easily and more 631 quickly than the common procedure of EEM matrices by developing PARAFAC models 632 before the classification and regression models. PARAFAC has the advantage of providing 633 more information about the fluorescent compounds presented in the matrices, yet it 634 involves a more complex chemometric approach.

635 The addition of grape-must caramel is a common practice in the vinegar industry. It has 636 not been studied previously because it was thought that it had no influence on the final 637 vinegars. However, sensory changes in vinegars caused by adding grape-must caramel 638 were also studied. The results show that low concentrations produce changes in the

639 organoleptic characteristics of PDO wine vinegars, reaffirming the relevance of
640 determining the addition of grape-must caramel.

641 This study opens up a new means of detecting and monitoring the addition of grape-must
642 caramel to wine vinegar, thus preventing unfair competition between wineries and brands,
643 as well as preventing potential adulterations related to the addition of grape-must caramel.
644 Therefore, now that the important effects that adding grape-must caramel has upon a PDO
645 vinegar's final quality have been demonstrated, further studies are needed in order to gain
646 greater knowledge of the subject with the aim of establishing a limit or creating a
647 monitoring protocol regarding the addition of grape-must caramel to PDO vinegars.

648 **5. ACKNOWLEDGEMENTS**

649 This work was supported by "Consejería de Economía, Innovación y Ciencia, Junta de
650 Andalucía" [P12-AGR-1601]; and the FPU scholarship of "Ministerio de Educación, Cultura
651 y Deporte" [FPU014/01247]. The authors would like to thank the Spanish Regulatory
652 Councils of the wine vinegar PDOs for their invaluable help with the acquisition of the
653 samples. Moreover, authors are also grateful for the members of the tasting panel who
654 participated in the study voluntarily.

6. REFERENCES

655 Airado-Rodríguez, D., Durán-Merás, I., Galeano-Díaz, T., & Wold, J. P. (2011). Front-face
656 fluorescence spectroscopy: A new tool for control in the wine industry. *Journal of*
657 *Food Composition and Analysis*, 24(2), 257-264.
658 <https://doi.org/10.1016/j.jfca.2010.10.005>

659 Arancibia, J. A., Damiani, P. C., Escandar, G. M., Ibañez, G. A., & Olivieri, A. C. (2012). A
660 review on second- and third-order multivariate calibration applied to chromatographic
661 data. *Journal of Chromatography B: Analytical Technologies in the Biomedical and*

662 *Life Sciences*, 910, 22-30. <https://doi.org/10.1016/j.jchromb.2012.02.004>

663 Azcarate, S. M., Araújo, A. De, Alcaraz, M. R., Ugulino, M. C., Araújo, D., Camiña, J. M., &
664 Goicoechea, H. C. (2015). Modeling excitation- emission fluorescence matrices with
665 pattern recognition algorithms for classification of Argentine white wines according, 666
184, 214-219.

667 Azcarate, S. M., Teglia, C. M., Karp, F., Camiña, J. M., & Goicoechea, H. C. (2017). A
668 novel fast quality control strategy for monitoring spoilage on mayonnaise based on
669 modeling second-order front-face fluorescence spectroscopy data. *Microchemical*
670 *Journal*, 133, 182-187. <https://doi.org/10.1016/j.microc.2017.03.036>

671 Bro, R. (1996). Multiway calibration. Multilinear PLS. *Journal of Chemometrics*, 10(1), 47-
672 61. [https://doi.org/10.1002/\(SICI\)1099-128X\(199601\)10:1<47::AID-
673 CEM400>3.0.CO;2-C](https://doi.org/10.1002/(SICI)1099-128X(199601)10:1<47::AID-CEM400>3.0.CO;2-C)

674 Bro, R. (1997). PARAFAC. Tutorial and applications. *Chemometrics and Intelligent*
675 *Laboratory Systems*, 38(2), 149-171. [https://doi.org/10.1016/S0169-7439\(97\)00032-4](https://doi.org/10.1016/S0169-7439(97)00032-4)

676 Bro, R. (1998). Multi-way analysis in the food industry. Models, algorithms, and
677 applications., (1998).

678 Bro, R., & Kiers, H. A. L. (2003). A new efficient method for determining the number of
679 components in PARAFAC models. *Journal of Chemometrics*, 17(5), 274-286.
680 <https://doi.org/10.1002/cem.801>

681 Callejón, R. M., Amigo, J. M., Pairo, E., Garmón, S., Ocaña, J. A., & Morales, M. L. (2012).
682 Classification of Sherry vinegars by combining multidimensional fluorescence,
683 parafac and different classification approaches. *Talanta*, 88, 456-462.
684 <https://doi.org/10.1016/j.talanta.2011.11.014>

685 Capuano, E., & Fogliano, V. (2011). Acrylamide and 5-hydroxymethylfurfural (HMF): A
686 review on metabolism, toxicity, occurrence in food and mitigation strategies. *LWT -*
687 *Food Science and Technology*, 44(4), 793-810.
688 <https://doi.org/10.1016/j.lwt.2010.11.002>

689 Casale, M., Pasquini, B., Hooshyari, M., Orlandini, S., Mustorgi, E., Malegori, C., ...
690 Furlanetto, S. (2018). Combining excitation-emission matrix fluorescence
691 spectroscopy, parallel factor analysis, cyclodextrin-modified micellar electrokinetic
692 chromatography and partial least squares class-modelling for green tea
693 characterization. *Journal of Pharmaceutical and Biomedical Analysis*, 159, 311-317.
694 <https://doi.org/10.1016/j.jpba.2018.07.001>

695 Christensen, J., Becker, E. M., & Frederiksen, C. S. (2005). Fluorescence spectroscopy
696 and PARAFAC in the analysis of yogurt. *Chemometrics and Intelligent Laboratory*
697 *Systems*, 75(2), 201-208. <https://doi.org/10.1016/j.chemolab.2004.07.007>

698 Council Regulation (EC) No 510/2006 of 20 March 2006 on the protection of geographical
699 indications and designations of origin for agricultural products and foodstuffs.

700 Danezis, G. P., Tsagkaris, A. S., Camin, F., Brusica, V., & Georgiou, C. A. (2016). Food
701 authentication: Techniques, trends & emerging approaches. *TrAC - Trends in*
702 *Analytical Chemistry*, 85, 123-132. <https://doi.org/10.1016/j.trac.2016.02.026>

703 Dufour, É., Letort, A., Laguet, A., Lebecque, A., & Serra, J. N. (2006). Investigation of
704 variety, typicality and vintage of French and German wines using front-face
705 fluorescence spectroscopy. *Analytica Chimica Acta*, 563(1-2 SPEC. ISS.), 292-299.
706 <https://doi.org/10.1016/j.aca.2005.11.005>

707 Elcoroaristizabal, S., Bro, R., García, J. A., & Alonso, L. (2015). PARAFAC models of
708 fluorescence data with scattering: A comparative study. *Chemometrics and Intelligent*

709 *Laboratory Systems*, 142, 124-130. <https://doi.org/10.1016/j.chemolab.2015.01.017>

710 Elcoroaristizabal, S., Callejón, R. M., Amigo, J. M., Ocaña-González, J. A., Morales, M. L.,
711 & Ubeda, C. (2016). Fluorescence excitation-emission matrix spectroscopy as a tool
712 for determining quality of sparkling wines. *Food Chemistry*, 206, 284-290.
713 <https://doi.org/10.1016/j.foodchem.2016.03.037>

714 García Parrilla, M. C., Heredia, F. J., & Troncoso, A. M. (1999). Sherry wine vinegars: 715
 Phenolic composition changes during aging. *Food Research International*, 32(6),
716 433-440. [https://doi.org/10.1016/S0963-9969\(99\)00105-2](https://doi.org/10.1016/S0963-9969(99)00105-2)

717 Heidari, S., Hemmateenejad, B., Yousefinejad, S., & Moosavi-Movahedi, A. A. (2018).
718 Excitation- emission matrix fluorescence spectroscopy combined with three-way
719 chemometrics analysis to follow denatured states of secondary structure of bovine
720 serum albumin. *Journal of Luminescence*, 203(December 2017), 90-99.
721 <https://doi.org/10.1016/j.jlumin.2018.06.029>

722 Karoui, R., & Blecker, C. (2011). Fluorescence Spectroscopy Measurement for Quality 723
 Assessment of Food Systems-a Review. *Food and Bioprocess Technology*, 4(3),
724 364-386. <https://doi.org/10.1007/s11947-010-0370-0>

725 Karoui, R., & De Baerdemaeker, J. (2007). A review of the analytical methods coupled with
726 chemometric tools for the determination of the quality and identity of dairy products.
727 *Food Chemistry*, 102(3), 621-640. <https://doi.org/10.1016/j.foodchem.2006.05.042>

728 Morales, M. L., Tesfaye, W., García-Parrilla, M. C., Casas, J. A., & Troncoso, A. M. (2002). 729
 Evolution of the aroma profile of sherry wine vinegars during an experimental aging in
730 wood. *Journal of Agricultural and Food Chemistry*, 50(11), 3173-3178.
731 <https://doi.org/10.1021/jf011313w>

732 Olivieri, A. C. (2014). Analytical figures of merit: From univariate to multiway calibration.
733 *Chemical Reviews*, 114(10), 5358-5378. <https://doi.org/10.1021/cr400455s>

734 Olivieri, A. C., & Escandar, G. M. (2014). *Practical Three-Way Calibration*. Elsevier.
735 <https://doi.org/https://doi.org/10.1016/C2012-0-07419-4>

736 Ortega-Heras, M., & González-Sanjosé, M. L. (2009). Binding capacity of brown pigments
737 present in special Spanish sweet wines. *LWT - Food Science and Technology*,
738 42(10), 1729-1737. <https://doi.org/10.1016/j.lwt.2009.04.001>

739 Öztürk, B., Ankan, A., & Özdemir, D. (2010). *Olive Oil Adulteration with Sunflower and 740*
Corn Oil Using Molecular Fluorescence Spectroscopy. Olives and Olive Oil in Health
741 *and Disease Prevention*. Elsevier Inc. [https://doi.org/10.1016/B978-0-12-374420-](https://doi.org/10.1016/B978-0-12-374420-742)
742 3.00050-4

743 Palacios, V., Valcarcel, M., Caro, I., & Perez, L. (2002). Chemical and biochemical
744 transformations during the industrial process of sherry vinegar aging. *J Agric Food*
745 *Chem*, 50(15), 4221-4225. <https://doi.org/10.1021/jf020093z>

746 Ríos-Reina, R., Elcoroaristizabal, S., Ocaña-González, J. A., García-González, D. L.,
747 Amigo, J. M., & Callejón, R. M. (2017). Characterization and authentication of
748 Spanish PDO wine vinegars using multidimensional fluorescence and chemometrics.
749 *Food Chemistry*, 230, 108-116. <https://doi.org/10.1016/j.foodchem.2017.02.118>

750 Sádecká, J., & Tóthová, J. (2007). Fluorescence Spectroscopy and Chemometrics in the
751 Food Classification- a Review. *Czech J. Food Sci. Vol*, 25(4), 159-173. Retrieved
752 from <http://www.journals.uzpi.cz/publicFiles/00302.pdf>

753 Sáiz-Abajo, M. J., González-Sáiz, J. M., & Pizarro, C. (2006). Prediction of organic acids
754 and other quality parameters of wine vinegar by near-infrared spectroscopy. A

755 feasibility study. *Food Chemistry*, 99(3), 615-621.
756 <https://doi.org/10.1016/j.foodchem.2005.08.006>

757 Sayago, a, García-Gonzalez, D. L., Morales, M. T., & Aparicio, R. (2007). Detection of the
758 presence of refined hazelnut oil in refined olive oil by fluorescence spectroscopy.
759 *Journal of Agricultural and Food Chemistry*, 55(6), 2068-2071.
760 <https://doi.org/10.1021/jf061875l>

761 Tesfaye, W., Morales, M. L., Callejón, R. M., Cerezo, A. B., González, A. G., García- 762
Parrilla, M. C., & Troncoso, A. M. (2010). Descriptive Sensory Analysis of Wine
763 Vinegar: Tasting Procedure and Reliability of New Attributes. *Journal of Sensory*
764 *Studies*, 25(2), 216-230. <https://doi.org/10.1111/j.1745-459X.2009.00253.x>

765 Vigneau, E., Qannari, E. M., Jaillais, B., Mazerolles, G., & Bertrand, D. (2006). Méthodes
766 prédictives. In D. Bertrand & E. Dufour (Eds.), *La spectroscopie infrarouge et ses 767*
applications analytiques (Lavoisier, pp. 347-397). Paris.

768 Zhu, D., Ji, B., Eum, H. L., & Zude, M. (2009). Evaluation of the non-enzymatic browning in
769 thermally processed apple juice by front-face fluorescence spectroscopy. *Food*
770 *Chemistry*, 113(1), 272-279. <https://doi.org/10.1016/j.foodchem.2008.07.009>

771 Zhu, L., Wu, H. L., Xie, L. X., Fang, H., Xiang, S. X., Hu, Y., ... Yu, R. Q. (2016). A
772 chemometrics-assisted excitation-emission matrix fluorescence method for 773
simultaneous determination of arbutin and hydroquinone in cosmetic products.
774 *Analytical Methods*, 8(24), 4941-4948. <https://doi.org/10.1039/c6ay00821f>

FIGURE CAPTIONS

Fig.1. Fluorescence landscapes in the form of contour plots and PARAFAC loadings (excitation/emission profiles) of each main fluorophore of different sets of samples: Calibration curves made with the Crianza “Control” wine vinegars as matrix from both PDOs (a); All the samples from both PDOs (modified and Unmodified) (b); Grape-must caramel calibration curve made with the hydroacetic matrix ((c) and (d)).

Fig.2. Score and loading plots of the principal components obtained by a PCA by using the extracted PARAFAC factors with all the Modified (MOD) and Unmodified (UNMOD) samples: for “Vinagre de Montilla-Moriles” PDO (a); for “Vinagre de Jerez” PDO (b).

Fig.3. Chromatograms corresponding to different solutions of grape-must caramel in the hydroacetic matrix showing the elution of the selected peaks (a); linear regression curves of the three compounds selected (5-HMF and two unknowns) obtained by the different percentages of grape-must caramel in hydroacetic matrix (b). HGMC= Hydroacetic matrix with the addition of grape-must caramel.

Fig.4. Figures of merit of the multiway calibration models developed with the grape-must calibration curves of both PDO considered together (a) and for each PDO individually ((b) and (c)).

SUPPLEMENTARY MATERIAL

Fig. 1. Schematic representation of the different samples and grape-must caramel curves included in the study.

Fig. 2. Plot of the variance explained (%), core consistency (%), number of iterations and time to carried out each model, by extracting from 1 to 6 factors, used in the selection of the best number of factors for the Vinagre de Jerez and Vinagre de

Montilla-Moriles (modified and unmodified samples) PARAFAC models, and for the PARAFAC model made with the grape-must caramel calibration curve in hydroacetic matrix.

Fig. 3. Evolution of the scores of PARAFAC factors extracted from the hydroacetic curve with the addition of grape-must caramel.

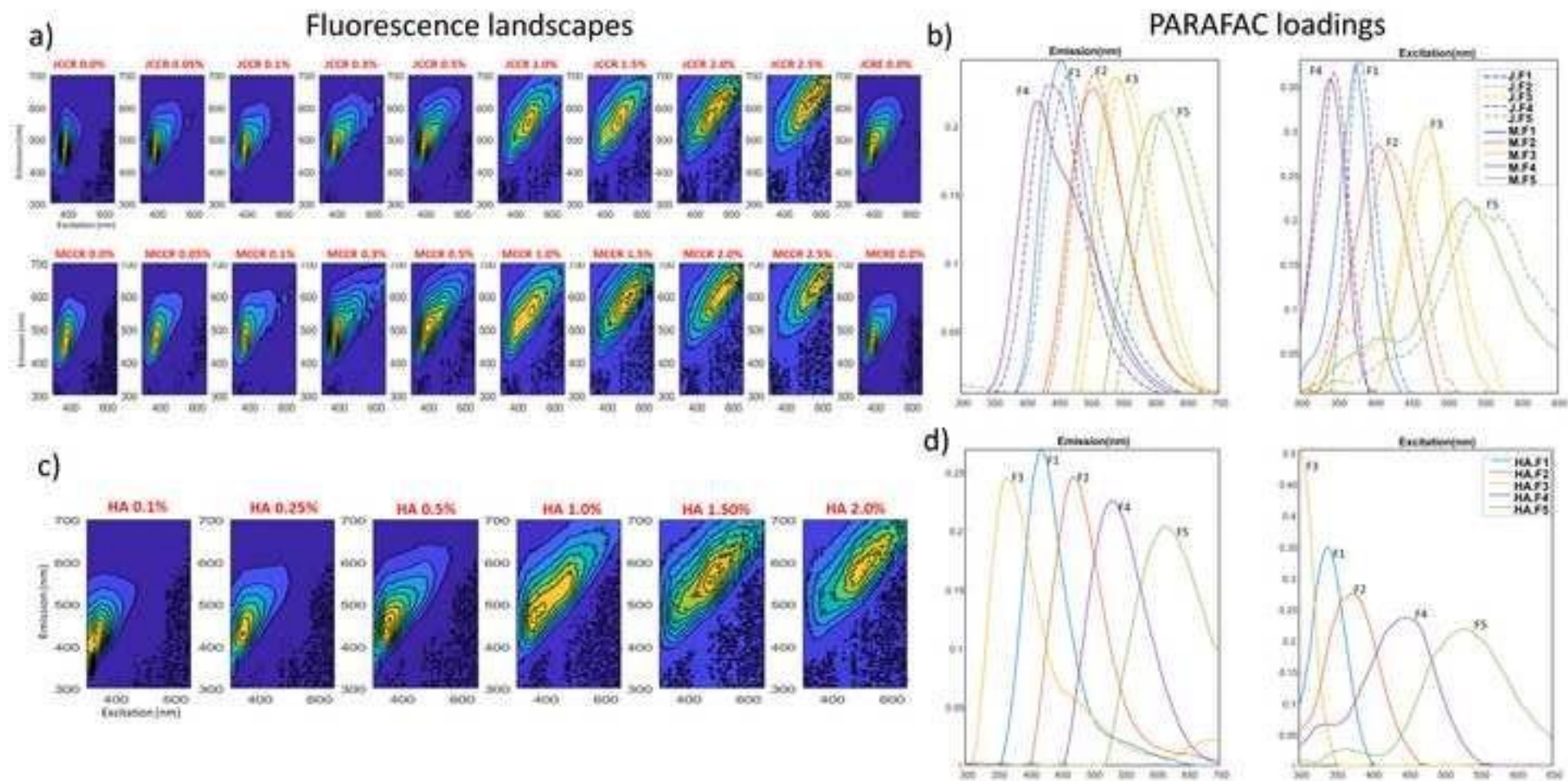
Table 1. Samples included in the study.

Class		Unmodified		Modified (curves made by addition of grape-must caramel)		TOTAL
		Control samples (without caramel)	Commercial samples (possibility of having caramel)	Control matrix (0.05, 0.10, 0.20, 0.30, 0.40, 0.50, 0.75, 1.00, 1.25, 1.50, 1.75, 2.00, 2.50 % v/v)	Commercial matrix (0.05, 0.10, 0.30, 0.50, 1.00, 1.50, 2.00, 2.50 % v/v)	
“Vinagre de Jerez”	Crianza (JCR)	1 (JCCR)	10 (JCR)	13	8	32
	Reserva (JRE)	1 (JCRE)	13 (JRE)	13	-	27
“Vinagre de Montilla- Moriles”	Crianza (MCR)	1 (MCCR)	6 (MCR)	13	8	28
	Reserva (MRE)	1 (MCRE)	5 (MRE)	13	-	19
6% Hydroacetic matrix (HA)		-	-	6 (0.10, 0.25, 0.50, 1.00, 1.50, 2.00%)		6
Total		38		74		112

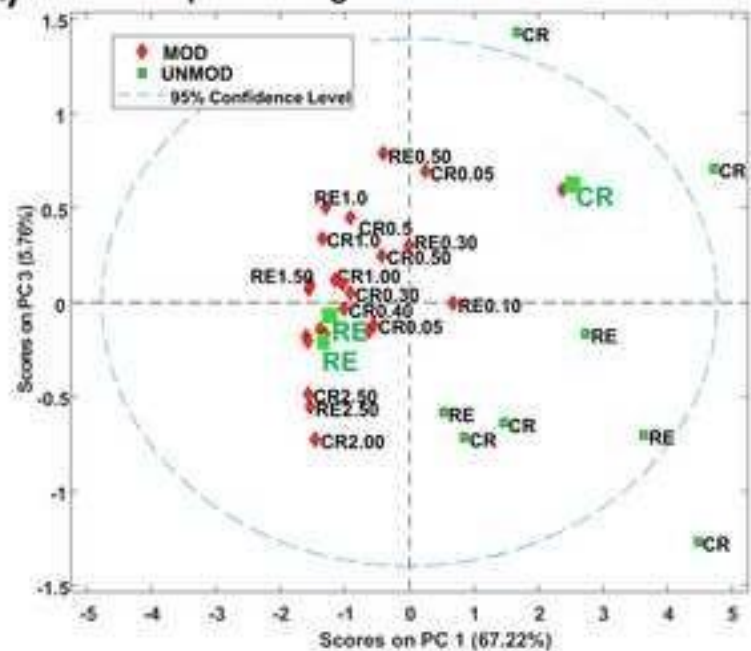
Table 2. PLS-DA and NPLS-DA classification results using the PARAFAC components and the EEMs, respectively.

PDO	LVs		% TOTAL EXPLAINED VARIANCE		Training	% Correct Classification		SAMPLES MISSCLASSIFIED	
	P	N	P	N		P	N	P	N
"Vinagre de Jerez"	4	3	99.7	99.7	Modified	100	100	0	0
					Unmodified	100	100	0	0
					Prediction	% Correct Classification		SAMPLES MISSCLASSIFIED	
						P	N	P	N
					Modified	100	100	0	0
Unmodified	42.86	71.43	4 (2RE,2CR)	3 (2RE,1CR)					
"Vinagre de Montilla-Moriles"	3	3	96.8	96.8	Training	% Correct Classification		SAMPLES MISSCLASSIFIED	
						P	N	P	N
					Modified	100	100	0	0
					Unmodified	100	100	0	0
					Prediction	% Correct Classification		SAMPLES MISSCLASSIFIED	
						P	N	P	N
Modified	100	100	0	0					
Unmodified	25	40.00	3 (2RE,1CR)	3 (2RE,1CR)					
Both PDOs together	5	3	99.6	99.1	Training	% Correct Classification		SAMPLES MISSCLASSIFIED	
						P	N	P	N
					Modified	90.70	89.47	4 (M<0.75%)	4 (M<0.75%)
					Unmodified	86.36	90.90	3 (2JRE,1JCR)	2 (1JRE,1JCR)
					Prediction	% Correct Classification		SAMPLES MISSCLASSIFIED	
						P	N	P	N
Modified	100	100	0	0					
Unmodified	36.36	58.33	7 (4J, 3M)	5 (3J,2M)					

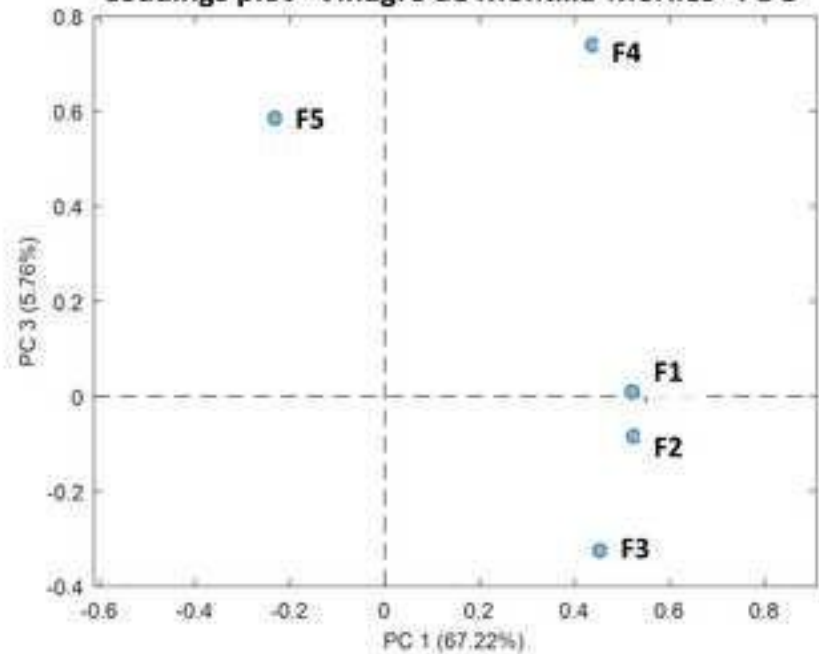
*Note: P= PLS-DA model; N= NPLS-DA model. LVs= Latent variables.



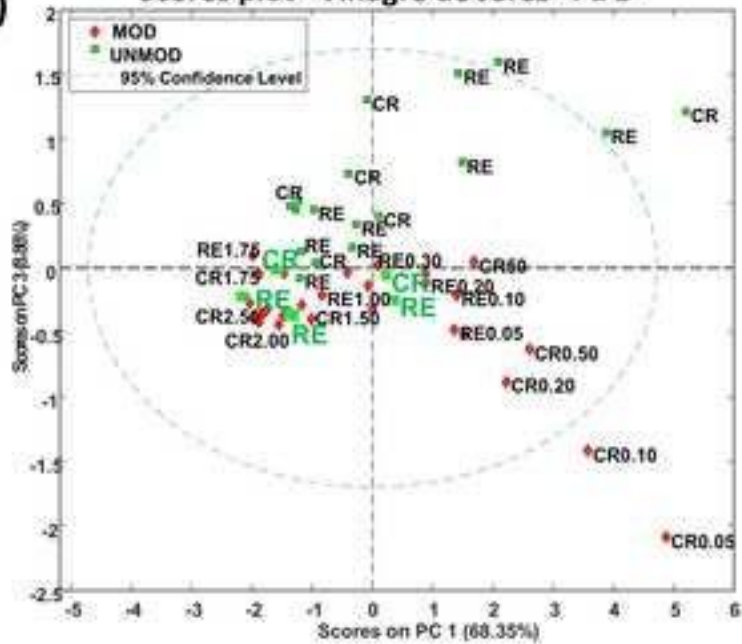
A) Scores plot "Vinagre de Montilla-Moriles" PDO



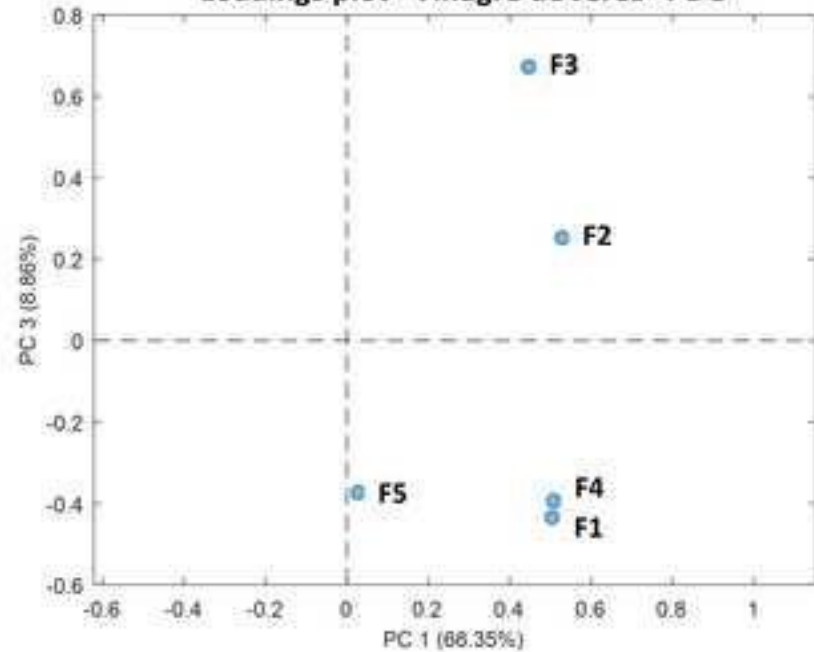
Loadings plot "Vinagre de Montilla-Moriles" PDO



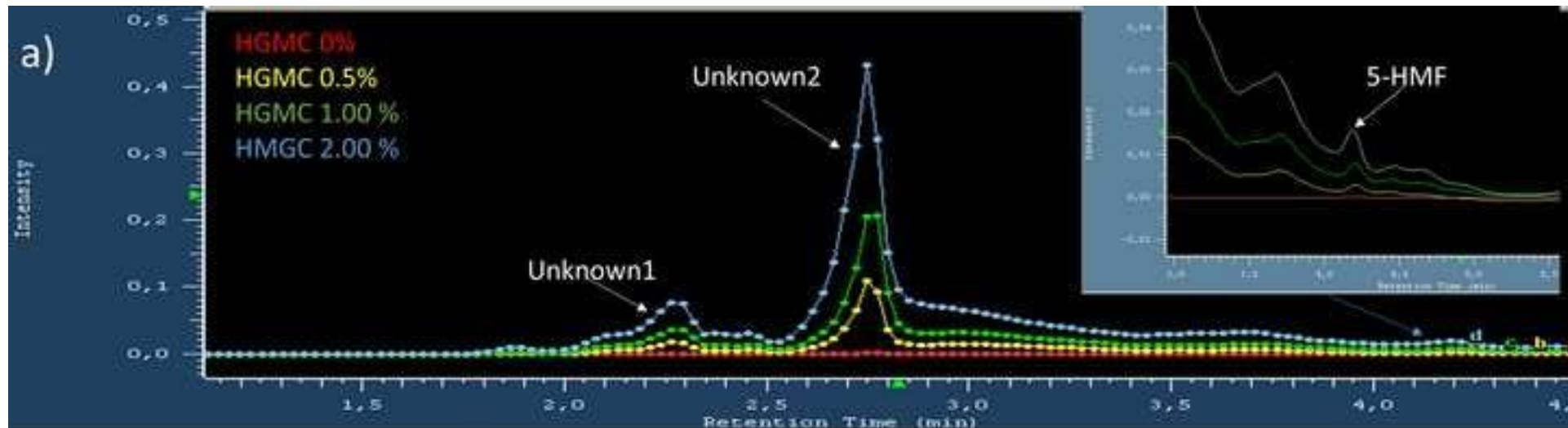
B) Scores plot "Vinagre de Jerez" PDO



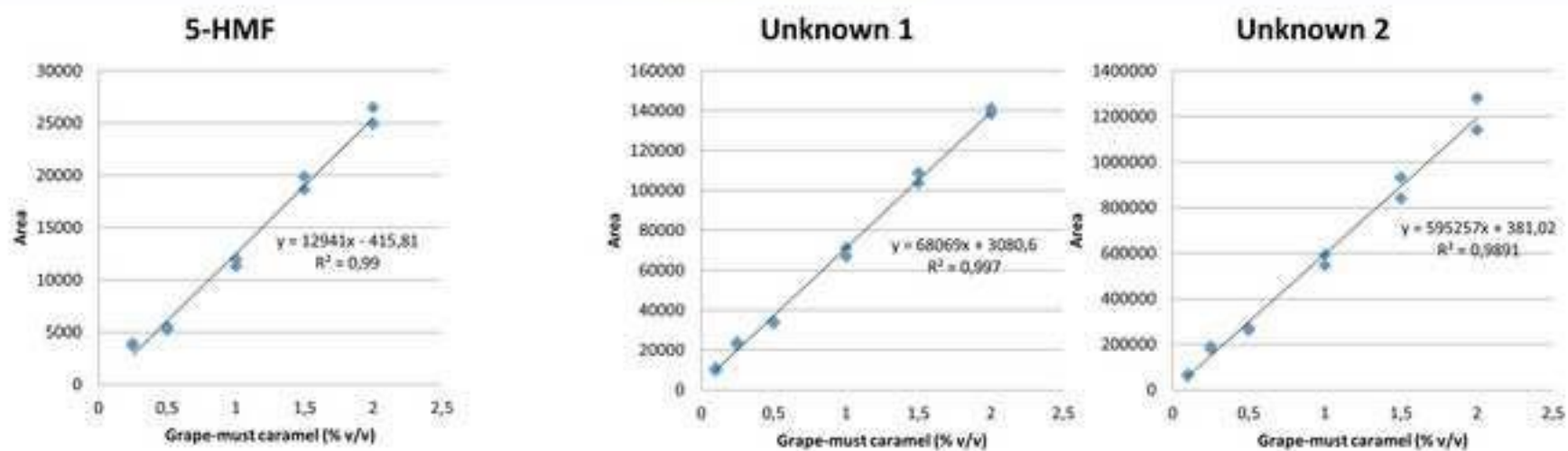
Loadings plot "Vinagre de Jerez" PDO



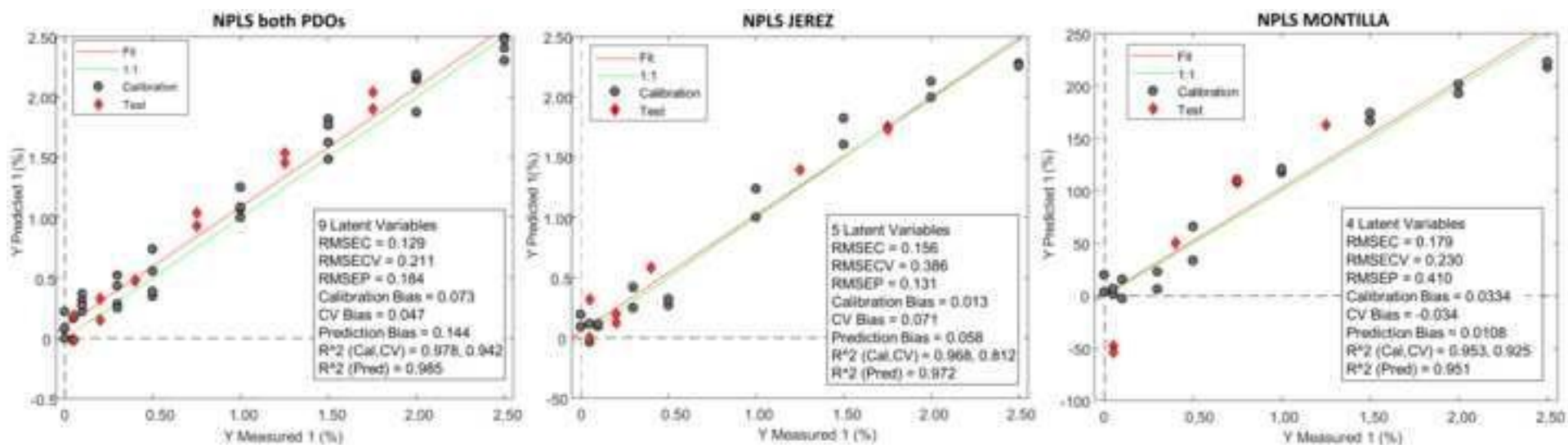
Figure(s)



b)



Figure(s)



Supplementary Material

[Click here to download Supplementary Material: Supplementary Fig 1.tif](#)

Supplementary Material

[Click here to download Supplementary Material: Supplementary Fig 2-new.tif](#)

Supplementary Material

[Click here to download Supplementary Material: Supplementary Fig 3-rev.tif](#)

Supplementary Material

[Click here to download Supplementary Material: Supplementary material Table 1 new.docx](#)

Supplementary Material

[Click here to download Supplementary Material: supplementary material-Table 2-rev.docx](#)